CA8507988

TRI-PP-85-9
Feb 1985

Polarized Proton Induced Pion Production on ^{10}B at 200, 225, 250 and 260 MeV Incident Energies

W. Ziegler, E.G. Auld, W.R. Falk[†], G.L. Giles, G. Jones, G.J. Lolos[*], E. McParland

Physics Department, University of British Columbia, Vancouver, B.C., Canada V6T 2A6

P.L. Walden and D.F. Ottewell

TRIUMF, 4004 Wesbrook Mall Vancouver B.C., Canada V6T 2A6

The angular distributions of both the differential cross-section and the analyzing power are presented for the $^{10}B(\vec{p},\pi^+)^{11}B$ reaction leading to the ground and first excited states of ^{11}B. The differential cross-section shows very little angular structure or energy dependence, but the analyzing power exhibits a considerable energy dependence for both states. This dependence, similar to that observed for the $^{12}C(\vec{p},\pi^+)^{13}C$ reaction, may be a signature of the fact that single-particle final states are involved.

(Submitted to Physical Review C Rapid Communications)

[†]Permanent address: Physics Department, University of Manitoba, Winnipeg, Manitoba, Canada R3T 2N2

[*]Now with the Department of Physics and Astronomy, University of Regina, Regina, Saskatchewan, Canada S4S 0A2

For some time now, there has been the expectation that proton-induced pion production reactions, $A(p,\pi^+)A+1$, would constitute a useful spectroscopic tool for the investigation of high momentum components of nuclear wave functions once the production process itself was sufficiently well understood. As a result, reactions of this type have attracted considerable attention over the past several years.[1-3] So far, however, even though much data now exist, the basic production process is still unclear.

In the meantime, experiments have tended to look for systematic trends in the data for clues in understanding the basic reaction mechanism. One such clue could be the strong energy dependence of the analyzing power observed for the ground state transition of the $^{12}C(\vec{p},\pi^+)^{13}C$ reaction.[4] This strong dependence in contrast to the weak dependence osberved for $^{9}Be(\vec{p},\pi^+)^{10}Be_{g.s.}$ reaction,[5] encouraged us to investigate another even A nucleus.

In this communication the angular distributions of the analyzing power and differential cross-section for incident proton energies of 200, 225, 250 and 260 MeV are presented and compared to the corresponding situation in the other light nuclei. In this respect, a possible trend due to single-particle final states is pointed out.

The experiment was performed at the TRIUMF cyclotron using an extracted polarized beam of 20 and 30 nA intensity. The spin polarization of the beam was typically 75%. The beam intensity as well as its polarization were monitored using polarimeters based on p-p elastic scattering from thin CH_2 (polyethylene) targets.[6,7]

The areal thickness of the boron targets (all enriched to 92% ^{10}B), of the order of 100 mg/cm^2, were known to better than 1%. The background due to the 8% contamination of ^{11}B in the target was carefully checked. For the data presented here, where only the ground and first excited states are considered, the ^{11}B backgrounds in this region contributed less than 1% to the two states for all measurements.

The basic apparatus used to detect and identify the pions was a 65 cm Browne-Buechner[8] magnetic spectrograph. Three scintillators provided time-of-flight and energy-loss information as well as the event definition. The pion trajectory and thus the pion momentum was determined by three helically wound multi-wire proportional chambers.[9] A detailed description of the experimental arrangement is described elsewhere.[4,10]

The overall efficiency and acceptance of the spectrograph was calibrated relative to the known cross-sections of the $pp \rightarrow d\pi^+$ reaction.[11] In this case, the incident proton energy and pion angle were chosen so that the pion energy was identical to that investigated in the $^{10}B(\vec{p},\pi^+)^{11}B$ reaction. In addition, a Monte-Carlo simulation of the spectrograph was applied to the $A(\vec{p},\pi^+)A+1$ reaction to determine the line shape associated with the spectrograph. The generation of "tails" in the momentum distribution of a single line due to multiple pole-face scattering in the spectrography itself is a significant effect.[10] The reliability of the Monte-Carlo in modelling this effect was checked by comparison to the strong $pp \rightarrow d\pi^+$ line. The full details of the calibration are described in Ref. 10. The line shapes so determined were then used to fit the ^{11}B spectra. One example of a typical energy spectrum along with its fit is shown in Fig. 1.

The analyzing power $A_{NO}(\theta)$ and the spin-averaged (unpolarized) differential cross-section $d\sigma/d\Omega(\theta)$ were calculated using the relations:

$$A_{NO}(\theta) = \frac{d\sigma(\uparrow)/d\Omega - d\sigma(\downarrow)/d\Omega}{P(\downarrow)d\sigma(\uparrow)/d\Omega + P(\uparrow)d\sigma(\downarrow)/d\Omega} \tag{1}$$

and

$$\frac{d\sigma}{d\Omega}(\theta) = \frac{P(\uparrow)d\sigma(\downarrow)/d\Omega + P(\downarrow)d\sigma(\uparrow)/d\Omega}{P(\uparrow) + P(\downarrow)} \tag{2}$$

where P and $d\sigma/d\Omega$ are the magnitudes of the beam polarization and spin-dependent differential cross-section, respectively. The arrows indicate the spin direction according to the Madison convention.[12]

The results are shown in Figs. 2 and 3. In Fig. 2(a) the 200 MeV results from Ref. 13 are also shown. The absolute normalization of the two sets of data agree remarkably well. In this energy region there also exist some forward angle measurements at 250 MeV.[14] The results in Ref. 14, however, must be renormalized up by a factor of 1.9 for the transition to the ground state and up by a factor of 4.5 for the transition to the 2.12 MeV state in order to have agreement with the results reported in this work.

Only the relative uncertainties are indicated in the figures. In addition, there is an overall systematic uncertainty of ~10% for the differential cross-sections and ~2% for the analyzing powers. The relative error consists of both the counting statistics and the random fluctuations in the beam current measurements (mainly due to the wrinkling of the thin polarimeter targets). The majority of the systematic uncertainty in the differential cross-section arises from the uncertainty in the calibration of the effective solid angle of the spectrograph. The systematic uncertainty assigned to the effective solid angle is mainly caused by systematic uncertainties in the $pp \rightarrow d\pi^+$ cross-sections and absolute beam current normalization. The systematic uncertainty of the analyzing powers is due to the uncertainty in the analyzing power of the polarimeters.

The differential cross-section show very little structure, although there may be a slight change in slope for the forward angle cross-sections for both states occurring between 225 and 250 MeV incident proton energy. The analyzing powers however show a considerable energy dependence for both states. Comparison of these results to that from other $A(\vec{p},\pi^+)A+1$ reactions [$^{9}Be(\vec{p},\pi^+)^{10}Be$ [5] and $^{12}C(\vec{p},\pi^+)^{13}C$ [4]] should help define the general trends associated with pion production. For example, the analyzing powers for transitions to both the ground and first excited states of ^{10}Be as well as the 9.5 MeV excited state of ^{13}C show very little energy dependence, whereas for transitions to the ground and first excited states of ^{11}B as well as to the ground state of ^{13}C, a very strong (and similar) dependence is observed. A demonstration of this trend is shown in Fig. 3(a).

A possible interpretation of the energy dependence in the latter case might be that of specific effects associated with single-particle final states.[15] Since the analyzing powers depend principally on spin-orbit coupling, it seems plausible that final states consisting of more than one particle ($^{10}Be_{g.s.}$, $^{10}Be_{3.37\ MeV}$, $^{13}C_{9.5\ MeV}$) would be candidates of an averaging effect and thus exhibit a "smoothed out" energy dependence. On the other hand, single particle final states (like $^{13}C_{g.s.}$) could be expected to manifest a strong energy dependent analyzing power. The $^{11}B_{g.s.}$ state, a single-hole state, would be expected to act like a single-particle state. The $^{11}B_{2.12\ MeV}$ state, a two-hole one-particle state, also shows this strong single-particle energy dependence. Since particles (including holes) like to couple to zero spin, it would not be unreasonable to expect the 2.12 MeV state of ^{11}B to act as an effective single-particle state. In order to determine whether the effects observed are truly signatures of single-particle final states, additional nuclei should be studied. In particular, we suggest analyzing power measurements of $^{16}O(\vec{p},\pi^+)^{17}O$ and $^{40}Ca(\vec{p},\pi^+)^{41}Ca$ reactions leading to low lying states which should exhibit a behaviour similar to that of $^{10}B(\vec{p},\pi^+)^{11}B$.

The assistance of Mr. R. Igarashi and Mrs. D. Sample in the data handling and analysis is very much appreciated. This work was supported in part by an NSERC grant.

References

1. B. Hoistad, Adv. in Nucl. Phys., Vol. II, ed. J.W. Negele and E. Vogt (Plenum, New York, 1979) p. 135.
2. D.F. Measday and G.H. Miller, Ann. Rev. in Nucl. and Part. Sci., 29, 121 (1979).
3. H.W. Fearing, Prog. in Part. and Nucl. Phys., vol. 7, ed. D. Wilkinson (Pergamon, New York, 1981) p. 113.
4. G.J. Lolos, E.G. Auld, W.R. Falk, G.L. Giles, G. Jones, B.J. McParland, R.B. Taylor, and W. Ziegler, Phys. Rev. C30, 574 (1984).
5. E.G. Auld, G. Jones, G.J. Lolos, E.L. Mathie, P.L. Walden and R.B. Taylor, Phys. Rev. C25, 2222 (1982).
6. L.G. Greeniaus and J. Soukup, TRIUMF Internal Report TRI-DNA-81-1 (1981).
7. D.V. Bugg, J.A. Edgington, C. Amsler, R.C. Brown, C.J. Oram, K. Shakarchi, N.M. Stewart, G.A. Ludgate, A.S. Clough, D.Axen, S. Jaccard and J. Vávra, J. Phys. G4, 1025 (1978).
8. C.P. Browne, and W.W. Buechner, Rev. Sci. Instr. 27, 899 (1959).
9. D.M. Lee, S.E. Sobottka and H.A. Thiessen, Nucl. Instrum. Methods 120, 153 (1974).
10. W. Ziegler, M.Sc. Thesis, University of British Columbia, 1983 (unpublished).
11. G. Jones, Workshop on Pion Production and Absorption in Nuclei, ed. R.D. Bent, AIPCP #79 (AIP, New York, 1982), p. 15.
12. Proc. 3rd Int. Symp. on Polarization Phenomena in Nuclear Reactions, Madison, Wisconsin, 1970, ed. H.H. Barschall and W. Haeberli (Univ. of Wisconsin, Madison, 1971).

13. P.H. Pile, R.D. Bent, R.E. Pollock, P.T. Debevec, R.E. Marrs, M.C. Green, T.P. Sjoreen, and F. Soga, Phys. Rev. Lett., 42 1461 (1979).

14. P. Couvert, Workshop on Pion Production and Absorption in Nuclei, ed. R.D. Bent, AIPCP #79 (AIP, New York, 1982), p. 187.

15. J. Iqbal, private communication (1984).

TABLE I

T_p (MeV)	$^{10}B(\vec{p},\pi^+)^{11}B_{g.s.}$			$^{10}B(\vec{p},\pi^+)^{11}B_{2.12\ MeV}$		
	θ_{cm} (Deg.)	$d\sigma/d\Omega_{cm}$ (nb/sr)	A_{NO}	θ_{cm} (Deg.)	$d\sigma/d\Omega_{cm}$ (nb/sr)	A_{NO}
200	49.8	471.(30.)	-0.222(.032)	49.9	130.0(9.8)	-0.451(.059)
	64.6	339.(22.)	-0.372(.034)	64.6	104.3(8.1)	-0.428(.061)
	74.9	196.(13.)	-0.475(.032)	75.0	55.6(4.3)	-0.694(.056)
	85.2	91.4(6.6)	-0.459(.046)	85.2	38.5(3.3)	-0.607(.067)
	95.2	94.7(6.5)	-0.329(.041)	95.3	36.1(2.9)	-0.586(.061)
	110.0	50.7(3.5)	-0.191(.040)	110.1	25.5(1.9)	-0.533(.051)
	124.5	56.7(3.8)	-0.189(.036)	124.5	19.9(1.5)	-0.379(.059)
	138.6	47.3(3.2)	-0.187(.039)	138.7	18.1(1.4)	-0.468(.060)
225	49.8	593.(37.)	-0.305(.018)	49.8	172.(11.)	-0.432(.033)
	59.3	348.(27.)	-0.252(.058)	59.3	84.9(9.6)	-0.63(.10)
	64.4	285.(18.)	-0.368(.024)	64.4	90.5(6.1)	-0.473(.042)
	79.9	122.8(8.1)	-0.095(.036)	79.9	51.6(3.8)	-0.270(.054)
	87.1	98.2(7.8)	0.000(.073)	87.1	55.1(5.1)	-0.435(.094)
	95.0	75.0(4.9)	-0.041(.035)	95.1	39.5(2.8)	-0.318(.048)
	109.8	46.9(3.2)	0.053(.042)	109.9	32.4(2.3)	-0.218(.050)
	124.3	30.0(2.0)	-0.094(.043)	124.3	19.2(1.4)	-0.295(.053)
	138.5	42.9(2.9)	-0.327(.043)	138.5	34.1(2.4)	-0.457(.047)
250	49.6	539.(33.)	-0.021(.021)	49.7	114.0(7.9)	-0.064(.046)
	57.0	376.(24.)	-0.029(.024)	57.1	82.4(5.8)	-0.351(.049)
	64.4	257.(16.)	-0.004(.023)	64.4	62.2(4.3)	-0.343(.045)
	74.7	132.0(8.5)	0.082(.031)	74.7	40.5(3.0)	-0.201(.056)
	84.9	73.2(5.9)	0.287(.066)	84.9	29.1(3.1)	0.05(.11)
	95.0	38.2(2.5)	0.534(.034)	95.0	19.2(1.4)	0.163(.052)
	109.8	14.2(1.4)	0.386(.099)	109.8	10.1(1.1)	0.29(.12)
	124.2	14.1(1.2)	-0.289(.086)	124.3	7.00(.77)	0.43(.12)
	130.4	12.1(1.2)	-0.505(.087)	130.5	7.05(.83)	-0.04(.13)
	138.5	14.2(1.2)	-0.506(.075)	138.5	7.19(.77)	-0.28(.11)
260	49.7	580.(39.)	-0.033(.039)	49.7	130.(11.)	-0.079(.082)
	64.4	252.(16.)	0.048(.024)	64.4	61.9(4.3)	-0.225(.048)
	74.7	127.4(8.7)	0.262(.042)	74.7	38.6(3.2)	-0.322(.076)
	84.9	82.5(5.4)	0.377(.037)	85.0	43.3(3.1)	0.106(.053)
	95.0	53.0(4.3)	0.525(.065)	95.0	24.0(2.4)	0.541(.096)
	104.9	27.8(2.4)	0.493(.092)	104.9	16.9(1.7)	0.47(.12)
	114.6	16.1(1.5)	0.16(.10)	114.7	8.23(.97)	0.51(.13)
	124.3	15.1(1.5)	-0.36(.10)	124.3	8.5(1.0)	0.41(.14)
	138.5	10.6(1.2)	-0.47(.12)	138.5	8.8(1.1)	-0.43(.13)

A list of the values for the differential cross-sections and analyzing powers for $^{10}B(\vec{p},\pi^+)$ reaction leading to $^{11}B_{g.s.}$ and $^{11}B_{2.12\ MeV}$ states. The numbers in parentheses reflect relative uncertainties. Systematic errors are estimated as ~10% for the differential cross-sections and ~2% for the analyzing powers.

Figure Captions

Figure 1. Energy spectrum of π^+ produced at 50° c.m. from 225 MeV incident protons with spin down. Line shape fits for the first two states are shown by the solid line.

Figure 2. The differential cross-sections for the transition leading to (a) the $^{11}B_{g.s.}$ and (b) the $^{11}B_{2.12\ MeV}$. In (a) the 200 meV differential cross-sections results of Ref. 13 are also shown.

Figure 3. The $A_{NO}(\theta)$ are shown for the transition leading to (a) the $^{11}B_{g.s.}$ and (b) the $^{11}B_{2.12\ MeV}$. As well the 200 and 250 MeV A_{NO} results of Refs. 4 and 5 are shown in (a) to demonstrate the general trends seen in the energy dependence of A_{NO}. The lines serve only as a guide to the eye.

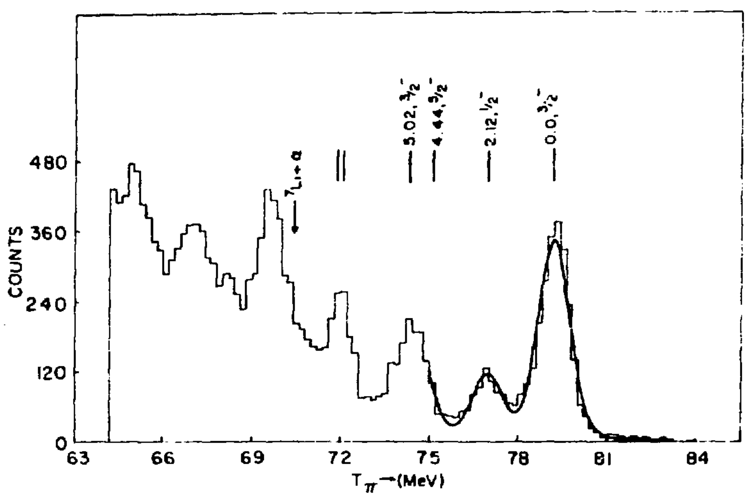

Fig. 1

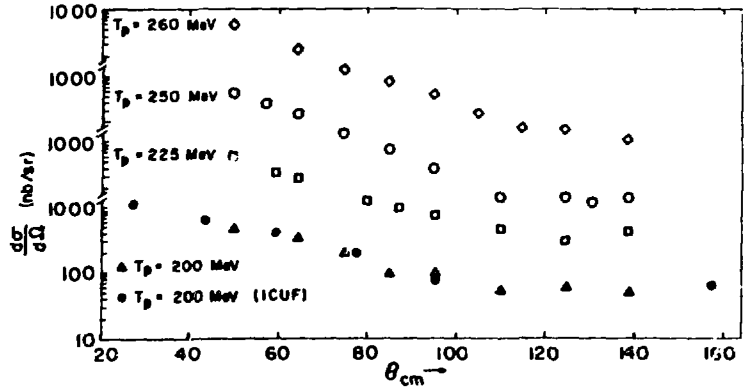
T_p = 260 MeV
T_p = 250 MeV
T_p = 225 MeV
T_p = 200 MeV
T_p = 200 MeV (ICUF)
$\frac{d\sigma}{d\Omega}$ (nb/sr)
θ_{cm}

Fig. 2a

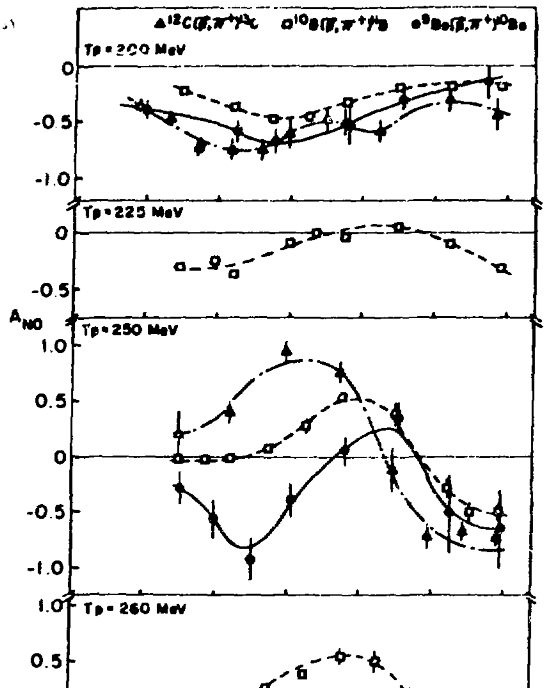
Tp = 200 MeV
Tp = 225 MeV
Tp = 250 MeV
Tp = 260 MeV
A_{NO}
θ_{cm}

Fig. 3a

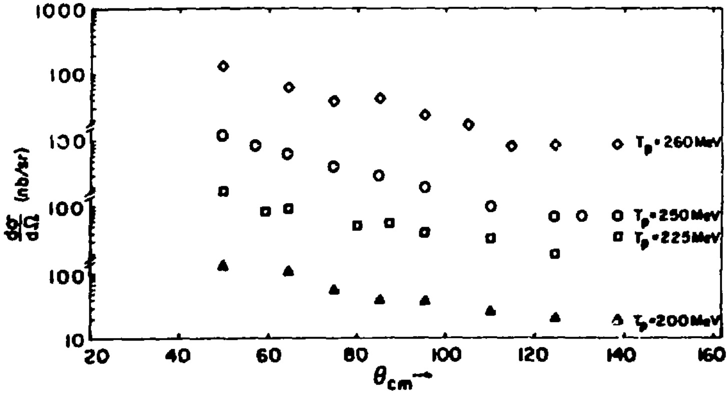

T_p=260MeV
T_p=250MeV
T_p=225MeV
T_p=200MeV
$\frac{d\sigma}{d\Omega}$ (nb/sr)
θ_{cm}

Fig. 2b

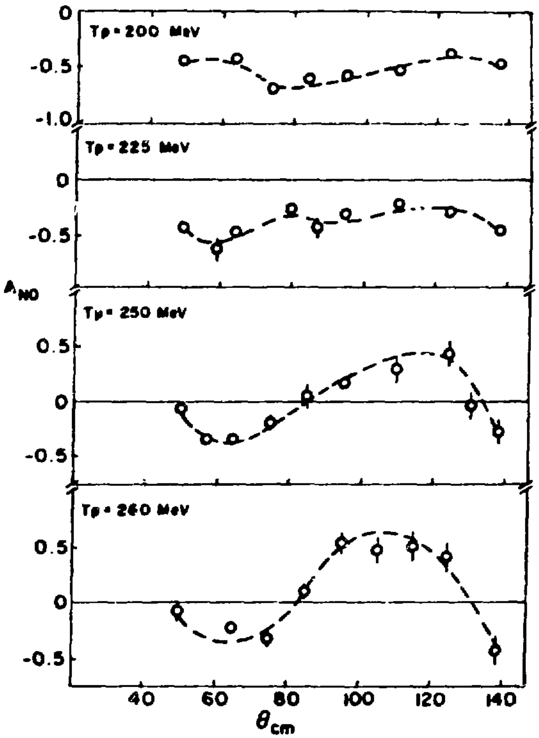

Tp = 200 MeV
Tp = 225 MeV
Tp = 250 MeV
Tp = 260 MeV
A_{N0}
θ_{cm}

Fig. 3b